INTERNATIONAL JOURNAL OF INTELLIGENT CONTROL AND SYSTEMS
VOL. 13, NO. 2, JUNE 2008, 136-145

Information-Theoretic Feature Detection and Its Application to Registration of Ultrasound Images

Zhe Wendy WANG, Greg SLABAUGH, Gozde UNAL and Tong FANG

***Abstract*—Medical ultrasound image registration is an essential component in an increasing number of applications, and has therefore been the subject of many studies in the literature. These applications use either generic registration algorithms or pixel-to-pixel comparison based ultrasound-specific methods. Hence, they are not well suited for the case of speckled images resulting from different realizations of a random process. To better handle the speckle, this work proposes an information-theoretic feature detector-based registration approach. Using speckle modeling based on the distributions of Rayleigh or normalized Fisher-Tippett, a speckle-specific information-theoretic feature detector is constructed and applied to provide feature images. Those feature images are then registered using differential equations, whose solution provides a transformation to bring the images into alignment. Compared to standard gradient-based techniques, the experimental results demonstrate the effectiveness of the proposed method, particularly for low contrast ultrasound images. It can be readily applied in the healthcare industry.**

***Index Terms*—image processing, speckled image, image registration, information theory**

1. INTRODUCTION

IMaging looks inside the patient's body, exposing the patient's anatomy beyond what is visible on the surface. Medical Imaging has a very successful history for medical diagnosis. Image registration, or motion estimation, is a fundamental problem in medical imaging and plays a crucial role in numerous clinical applications, including disease detection, analysis, and treatment. The images may be taken at different times, from different viewpoints, and/or different sensors, etc., and image registration seeks to recover the geometric transformation that brings the images into alignment.

In the recent decades, much literature has been devoted to the general problem of image registration and several good surveys [1], [2] as well as books [3], [4], [5] exist on the subject. To solve the registration problem, various methods have been proposed based on techniques such as iterative closest point (ICP) [6], feature matching [7], and intensity based similarity [8]. A recent research trend is the use of information theory to statistically model or compare images/image regions as well as differential equations [9], [10] to solve for the registration parameters. We adopt such an approach in this work. In addition, we note that recently there has been a renewed interest in gradient-based registration techniques [11], which are simple to implement in industrial applications and have numerous advantages over mutual-information based methods.

Medical ultrasound images are a very important diagnostic tool for physicians. Ultrasound is one of the most commonly used medical imaging modalities and has many advantages, as it is fast, portable, inexpensive and safe. However, speckle degrades severely the quality of medical B-mode ultrasonic images, and renders the registration of ultrasound speckled images as a difficult problem. Hence, the research targeting this problem is very important and has caught the increasing attentions in academia and industrial firms such as Siemens, GE and Philips. For example, Gardner *et al.* [12] developed a contrast quantification package as part of a medical ultrasound system. This package provided motion compensation through nonaffine image registration.

While generic image registration methods can be used to align ultrasound images, better results are attainable when one incorporates domain-specific knowledge into a registration algorithm. Ultrasound images are corrupted by speckle, which appears as a spatially correlated noise pattern, and its intensity distribution is well-known to be non-Gaussian. Indeed, fully formed speckle is known to be a multiplicative Rayleigh distribution in the envelope detected image and normalized Fisher-Tippett (doubly exponential) distribution in the log-compressed image (display image) [13].

By concealing fine structures, the speckle has a detrimental effect to the current image registration algorithms, especially those based on comparing images on a pixel-to-pixel basis.

For a fixed position of scatterers relative to the ultrasound beam, speckle is deterministic. Therefore, for small displacements, the speckle is correlated in one image to the next, and this fact has been used in speckle tracking methods [14]. However, if the displacement is large, or images are taken of the same region from different scans, or different transducers, etc., the correlation of the speckle will no longer exist. In such cases, registration algorithms that are based on comparing images on a pixel-to-pixel basis will have difficulty, since two corresponding pixels from the same anatomic structure can have very different intensity levels due to intensity variations of the speckle. Instead of comparing *samples* of normalized Fisher-Tippett distributions from one image to another, it would be preferable to compare estimates coming from the *distributions* instead. This is the novel method we take in our

The manuscript received on January 12, 2008; revised on May 1, 2008.
An early version of this paper was presented at the 2007 IEEE International Conference on Systems, Man and Cybernetics, Montreal, Canada, Oct. 2007.
Z. Wang is with the Department of Electrical and Computer Engineering, New Jersey Institute of Technology, Newark,NJ, 07102 USA (e-mail: zw27@njit.edu).
G. Slabaugh is with Medicsight PLC, London, U.K. (e-mail: greg_slabaugh@hotmail.com).
G. Unal is with Sabanci University, Istanbul, Turkey (e-mail: gozde.unal@siemens.com).
T. Fang is with Siemens Corporate Research,Princeton, NJ 08540,USA. (email: tong.fang@siemens.com).

approach.

While papers on ultrasound registration appear in the literature [15], many of these papers use generic registration algorithms. Ultrasound-specific registration algorithms [16], [17] are based on probability distributions that come from theoretical speckle models. The similarity metrics used in these papers rely on pixel-to-pixel intensity comparisons, which, for reasons given above, may not be desirable in many real-world applications due to the randomness of speckle.

Unlike such previous work, our proposed method relies on distribution-to-distribution comparisons. Consequently, it is significantly more robust. Our research proposes a registration scheme based on an information-theoretic detector for speckled medical images. In our previous work, we introduced analytic expressions for the J-divergence of Rayleigh and Fisher-Tippett distributed variables for comparing regions in an ultrasound image in the context of feature (edge) detection [19]. It is shown that this feature detector is more robust to speckle than other edge detection methods such as the derivative of Gaussian filter or the Canny edge detector, which are commonly used [20]. We use these feature detected images for registration. For each image to be registered, we first apply our information-theoretic feature detector to the image, producing a feature map that is robust to noise but still captures the significant edges in the image. We then register these feature maps using a sum of squared differences (SSD) similarity metric, which is used to guide differential equations that update the registration. Also, we extend it to the cases where the image speckle model is normalized Fisher-Tippett distributed since intensity of speckle is always non-negative, normalized Fisher-Tippett distribution is more suitable for speckle modeling in log-compressed images.

The rest of this paper is organized as follows. Section 2 introduces the statistical model of speckle. Section 3 describes our two-stage method. Section 4 provides results that demonstrate the ability of the proposed method to register ultrasound images, even for low contrast ultrasound images. By comparing with gradient-based techniques, the proposed method is shown to be much more robust in the presence of speckle. Section 5 concludes the paper by indicating the future research direction and the industrial applications of the proposed method.

2. PROBABILISTIC MODELING OF ULTRASOUND SPECKLE

Speckle is an interference pattern resulting from the coherent accumulation of random scattering in a resolution cell of the ultrasound beam. Fully formed speckle is typically assumed when the number of scatters per cell is greater than ten [13].

2.1. Rayleigh Case

It has been shown that the pixel intensity of the fully formed speckle in inphase/quadrature image, depicted in Fig. 1, $Q_I(x,y)$ at location (x,y), has a complex Gaussian distribution. The probability density function can be written as

$$p(Q_I) = \frac{1}{2\pi\sigma^2} e^{-|Q_I(x,y)|^2/(2\sigma^2)}. \quad (1)$$

Since Q_I is complex, its magnitude is taken to produce a real image. The distribution in this magnitude image $M(x,y)$ is Rayleigh [21],

$$p(M) = \frac{M(x,y)}{\sigma^2} e^{-M(x,y)^2/2\sigma^2}. \quad (2)$$

where $M(x,y)$ is real.

To obtain the maximum likelihood Rayleigh estimator, we differentiate the log likelihood of Eq.(2), with respect to σ, and set this expression to zero to determine the maximum likelihood estimate (MLE) of σ^2,

$$\sigma^2 = \frac{\int_\Omega M(x,y)^2 dxdy}{2\int_\Omega dxdy} \quad (3)$$

where Ω is a region in the image.

With the above equation, we can calculate the MLE of σ^2 from the image intensities in the region assuming Rayleigh distribution. Note that this distribution is fully described by this one parameter.

2.2. Normalized Fisher-Tippett Case

Let $I(x,y)$ denote a pixel intensity in the decorrelated log magnitude IQ image at the location (x,y), shown in Fig. 1. The probability density function (PDF) of normalized Fisher-Tippett for a pixel's intensity can be written as

$$p(I(x,y)) = 2e^{\frac{1}{2\sigma^2}} e^{\left(2I(x,y) - \ln 2\sigma^2 - e^{2I(x,y) - \ln 2\sigma^2}\right)}, \quad (4)$$

where σ^2 denotes the normalized Fisher-Tippett parameter of the reflectivity samples. For a region Ω in the image, the log likelihood can then be expressed as

$$\ell = \int_\Omega \left(\ln 2 + \frac{1}{2\sigma^2} + 2I(x,y) - \ln 2\sigma^2 - e^{2I(x,y) - \ln 2\sigma^2}\right) dxdy. \quad (5)$$

Next, we find an expression for σ^2 that is the maximum likelihood estimator of the normalized Fisher-Tippett distribution, by taking the derivative of ℓ and setting the expression equal to zero,

$$\frac{\partial \ell}{\partial \sigma} = \int_\Omega \left(-\frac{1}{\sigma^3} - \frac{4\sigma}{2\sigma^2} + \left(e^{2I(x,y) - \ln 2\sigma^2}\right) \frac{4\sigma}{2\sigma^2}\right) dxdy = 0. \quad (6)$$

We solve for σ^2 as

$$\sigma^2 = \frac{\int_\Omega (e^{2I(x,y)} - 1) dxdy}{2\int_\Omega dxdy}. \quad (7)$$

Thus, given a region Ω with area given by $\int_\Omega dxdy$, we can compute the maximum likelihood value of the normalized Fisher-Tippett distribution from the image intensities in the region.

3. INFORMATION-THEORETIC DETECTION BASED APPROACH

The proposed scheme consists of two major stages: first, using a feature detection method, we compute an edge map for each image to be registered. Next, we register the edge maps using differential equations.

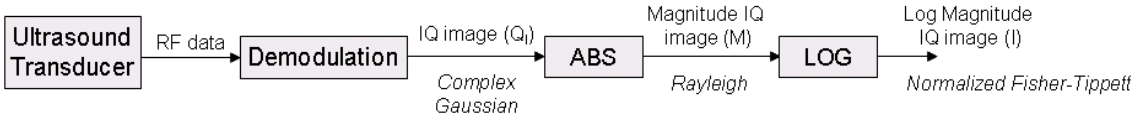

Fig. 1. Block diagram of ultrasound image formation process.

3.1. Feature detection

The feature detector we employ is based on a statistical comparison of regions in a speckle image. As mentioned above, fully formed speckle in the magnitude image can be modeled using a Rayleigh or normalized Fisher-Tippett distribution. The Rayleigh distribution has the form in Eq.(2), where σ^2 denotes the Rayleigh parameter of the reflectivity samples, while normalized Fisher-Tippett distribution is described in Eq.(4) and σ^2 fully describes the distribution.

Given a region Ω inside an ultrasound image, we can statistically estimate the Rayleigh distribution using the maximum likelihood estimator as in Eq.(3) and normalized Fisher-Tippett distribution using Eq.(7).

Our feature detector is based on information-theoretic comparison of two regions in an ultrasound image. That is, given two Rayleigh or normalized Fisher-Tippett distributions coming from different regions in the image, one parameterized by σ_1 and the other by σ_2, we compute the J-divergence, or symmetrized Kullback-Liebler distance, as a measure of the degree of difference between the distributions. The Kullback-Liebler distance of two distributions p and q is defined as

$$D(p||q) = \int p(x) \ln \frac{p(x)}{q(x)} dx. \tag{8}$$

Since it is not asymmetric, that is, $D(p||q) \neq D(q||p)$, one can symmetrize it using the J-divergence as

$$J = \frac{D(p||q) + D(q||p)}{2}. \tag{9}$$

For an image with Rayleigh distributions, we form a set of distributions (p_M, q_M) to model 2 unoverlapped windows of pixels, *i.e.*,

$$p_M(M) = \frac{M(x,y)}{\sigma_1^2} e^{-M(x,y)^2/2\sigma_1^2} \tag{10}$$

$$q_M(M) = \frac{M(x,y)}{\sigma_2^2} e^{-M(x,y)^2/2\sigma_2^2}, \tag{11}$$

where M is the intensity, and σ_1 and σ_2 are the parameters of each respective distribution.

Afterwards, we derive the expression for $D(p_M||q_M)$, from which $D(q_M||p_M)$ can be determined by symmetry to get the J-divergence,

$$D(p_M||q_M) = \int_0^\infty \frac{M}{\sigma_1^2} e^{-M^2/2\sigma_1^2} \ln \frac{\frac{M}{\sigma_1^2} e^{-M^2/2\sigma_1^2}}{\frac{M}{\sigma_2^2} e^{-M^2/2\sigma_2^2}} dM. \tag{12}$$

Expanding the logarithmic term yields

$$\begin{aligned} D(p_M||q_M) &= \int_0^\infty \frac{M}{\sigma_1^2} e^{-M^2/2\sigma_1^2} (\ln \frac{\sigma_2^2}{\sigma_1^2} - \frac{M^2}{2\sigma_1^2} + \frac{M^2}{2\sigma_2^2}) dM \\ &= \ln \frac{\sigma_2^2}{\sigma_1^2} \int_0^\infty \frac{M}{\sigma_1^2} e^{-M^2/2\sigma_1^2} dM \\ &\quad - \int_0^\infty \frac{M^3}{2\sigma_1^4} e^{-M^2/2\sigma_1^2} dM \\ &\quad + \int_0^\infty \frac{M^3}{2\sigma_1^2\sigma_2^2} e^{-M^2/2\sigma_1^2} dM \end{aligned} \tag{13}$$

which can be simplified as

$$D(p_M||q_M) = \ln\left(\frac{\sigma_2^2}{\sigma_1^2}\right) - 1 + \frac{\sigma_1^2}{\sigma_2^2}. \tag{14}$$

Therefore, the J-divergence of two Rayleigh distributed variables is derived as

$$J = -1 + \frac{\sigma_1^2}{2\sigma_2^2} + \frac{\sigma_2^2}{2\sigma_1^2}. \tag{15}$$

As stated above, the normalized Fisher-Tippett distribution models the intensities of fully formed speckle in the log magnitude image, which is typically presented to the user of an ultrasound machine. The normailized Fisher-Tippett distribution is given by Eq.(4). In this case, we model two regions with distributions p_I and q_I respectively, as

$$p_I(I(x,y)) = 2e^{\frac{1}{2\sigma_1^2}} e^{\left(2I(x,y) - \ln 2\sigma_1^2 - e^{2I(x,y) - \ln 2\sigma_1^2}\right)} \tag{16}$$

$$q_I(I(x,y)) = 2e^{\frac{1}{2\sigma_2^2}} e^{\left(2I(x,y) - \ln 2\sigma_2^2 - e^{2I(x,y) - \ln 2\sigma_2^2}\right)}, \tag{17}$$

where I is the intensity, and σ_1 and σ_2 denote normalized Fisher-Tippett parameters of the reflectivity samples.

Next, we derive an analytic expression for the Kullback-Liebler distance of two regions described by normalized Fisher-Tippett distributions, as

$$\begin{aligned} D(p_I||q_I) = &\int_0^\infty 2e^{\frac{1}{2\sigma_1^2}} e^{\left(2I - \ln 2\sigma_1^2 - e^{2I - \ln 2\sigma_1^2}\right)} \\ &\times \ln \frac{2e^{\frac{1}{2\sigma_1^2}} e^{\left(2I - \ln 2\sigma_1^2 - e^{2I - \ln 2\sigma_1^2}\right)}}{2e^{\frac{1}{2\sigma_2^2}} e^{\left(2I - \ln 2\sigma_2^2 - e^{2I - \ln 2\sigma_2^2}\right)}} dI \end{aligned} \tag{18}$$

Expending it gives

$$\begin{aligned} D(p_I||q_I) &= \frac{e^{\frac{1}{2\sigma_1^2}}}{\sigma_1^2} (\frac{1}{2\sigma_1^2} - \frac{1}{2\sigma_2^2} + \ln 2\sigma_2^2 - \ln 2\sigma_1^2) \\ &\quad \times \int_0^\infty e^{2I - e^{2I - \ln 2\sigma_1^2}} dI \\ &\quad + \frac{e^{\frac{1}{2\sigma_1^2}}}{\sigma_1^2} \int_0^\infty e^{2I - e^{2I - \ln 2\sigma_1^2}} \\ &\quad \times (e^{2I - \ln 2\sigma_2^2} - e^{2I - \ln 2\sigma_1^2}) dI \end{aligned} \tag{19}$$

After some mathematic operations, it can be simplified as

$$D(p_I||q_I) = \ln\left(\frac{\sigma_2^2}{\sigma_1^2}\right) - 1 + \frac{\sigma_1^2}{\sigma_2^2}. \quad (20)$$

Thus, the J-divergence of two Fisher-Tippett distributed variables is then

$$J = -1 + \frac{\sigma_1^2}{2\sigma_2^2} + \frac{\sigma_2^2}{2\sigma_1^2}. \quad (21)$$

Note that this is exactly the same expression for the J-divergence of two Rayleigh distributed variables. Eq.(21) is a similarity metric for ultrasound image registration of log magnitude IQ images.

The new feature detector has two sliding windows w_1 and w_2. They are placed on either side of a pixel. Given the set of pixels in w_1, Rayleigh or normalized Fisher-Tippett parameter σ_1^2 and σ_2^2 are determined using Eq.(3) or Eq.(7). Then, we compute J-divergence between these two distributions using Eq.(15) or Eq.(21) as a measure of how different the regions are. When the windows are placed to the left and to the right of the pixel, this gives a horizontal distance map $J_x(x,y)$ that is functionally similar to the gradient operator in the x direction, except that the values are non-negative. This can be repeated in the y direction. Here, we define a feature map $F(x,y)$ as

$$F(x,y) = \sqrt{J_x(x,y)^2 + J_y(x,y)^2}. \quad (22)$$

Figure 2 (c) shows an example of a cardiac ultrasound image and its feature map $F(x,y)$. Note that this feature detector is much less distracted by the speckle compared to the gradient estimator shown in (b), yet still detects the important edges in the image. The robustness of the feature detector comes from two sources: first, it compares distributions to distributions, rather than pixels to pixels, and second, it is based on integrals of the image and not derivatives. Taking derivatives of noisy data is often undesirable in image processing, as doing so emphasizes the noise. Integration, on the other hand, mitigates the effect of noise.

In the feature detection stage, each step, including computing MLE of σ^2 and J-divergence, takes constant time, given the window size. Therefore, the time complexity of the proposed feature detector is $O(WM)$, where W is the number of pixels within the sliding window and M is the number of pixels in the image. Hence, it is computationally efficient.

For each image to be registered, this feature detector is applied to transform the image into a feature-detected image that contains the important edges needed for registration while simultaneously mitigating false responses due to the speckle. These feature-detected images are then passed to the registration algorithm, to be described next.

3.2. Registration

We have investigated numerous similarity measures for the registration step. Among them, SSD was chosen as it offers sufficient accuracy and is very efficient.

Let $T(x,y)$ be the transformation between the two feature detected images, F_1 and and F_2. Our goal is to estimate the parameters of the transformation so that the feature images become aligned. To accomplish this, we minimize an energy function based on the sum of square differences between two feature maps,

$$E(T(x,y)) = \int [F_1(x,y) - F_2(T(x,y))]^2 \, dxdy. \quad (23)$$

where the transformation is applied to the second image. Starting with an initial guess, we can iteratively update the transformation using partial differential equations (PDEs) based on a Gauss-Newton optimization to minimize the energy functional in Eq.(23), described next.

First, we model the transformation of an image using three registration parameters, two translational components, $[t_x,\ t_y]^T$ and a rotation angle θ.

Let $\mathbf{g} = [t_x,\ t_y,\ \theta]^T$ be the current transformation, and $\delta\mathbf{g} = [\delta t_x,\ \delta t_y,\ \delta\theta]^T$ be a displacement of $\mathbf{g}$. Also, let $L = F_1(x,y) - F_2(T(x,y))$ come from the similarity metric. Then, by Taylor's theorem, we can write

$$L(\mathbf{g} - \delta\mathbf{g}) \approx L(\mathbf{g}) - \delta t_x \frac{\partial L}{\partial t_x} - \delta t_y \frac{\partial L}{\partial t_y} - \delta\theta \frac{\partial L}{\partial \theta}. \quad (24)$$

This equation tells us how much L decreases when the transformation parameters are perturbed by $\delta\mathbf{g}$.

From this, a set of simultaneous equations can be con-

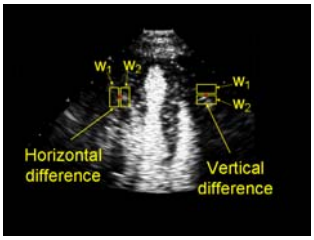

(a)

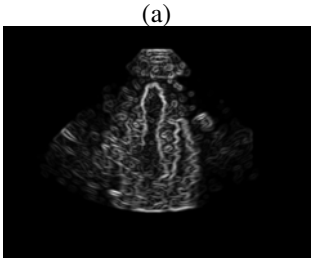

(b)

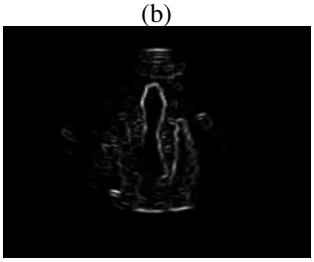

(c)

Fig. 2. Feature detection in a cardiac ultrasound image. Image (a), gradient (b), and J-divergence feature map (c) computed on the display image using the Fisher-Tippett method.

structed to minimize Eq.(23) as

$$\begin{pmatrix} \frac{\partial L_1}{\partial t_x} & \frac{\partial L_1}{\partial t_y} & \frac{\partial L_1}{\partial \theta} \\ \frac{\partial L_2}{\partial t_x} & \frac{\partial L_2}{\partial t_y} & \frac{\partial L_2}{\partial \theta} \\ \vdots & \vdots & \vdots \\ \frac{\partial L_M}{\partial t_x} & \frac{\partial L_M}{\partial t_y} & \frac{\partial L_M}{\partial \theta} \end{pmatrix} \begin{pmatrix} \delta t_x \\ \delta t_y \\ \delta \theta \end{pmatrix} = \begin{pmatrix} L_1 \\ L_2 \\ \vdots \\ L_M \end{pmatrix}. \quad (25)$$

where L_i denotes the difference between feature maps computed at pixel i, and M is the number of pixels in the image.

This overconstrained system of linear equations has the form $\mathbf{A}\delta\mathbf{g} = \mathbf{b}$, which can be solved using the pseudo-inverse as

$$\delta\mathbf{g} = (\mathbf{A}^T\mathbf{A})^{-1}\mathbf{A}^T\mathbf{b}. \quad (26)$$

We use $\delta\mathbf{g}$ in an iterative procedure, which at each step seeks to decrease the error. Upon convergence, the transformation is a local optimum of the energy.

The PDE is solved in a coarse-to-fine fashion using an image pyramid. Working in a multi-scale fashion is both more computationally efficient and helps prevent the solution from getting stuck in an undesirable local minimum.

4. EXPERIMENTAL RESULTS

Although there do exist speckled images that are not log-compressed, display ultrasound images usually go through a log-compression process. For completeness, we discuss the Rayleigh case in the above section. However, the experiments mainly focus on normalized Fisher-Tippett distribution as this is much commonly used in industry.

We begin with some experiments with synthetically generated data, designed to study the registration performance as the image contrast is diminished. There are two images at each contrast level. The images and their feature detection results are shown in Fig. 3. For comparison, a standard edge map formed with a difference of Gaussian filter is also created, which provides a smoothed implementation of the gradient. The ground truth registration parameters are $(2,3)$ for the translation and -5° for the rotation.

To quantify the performance of the feature detector, we use the contrast-to-noise ratio (CNR) to determine the detectability of edges in the feature maps. We define the contrast in the image as the difference of the mean value in the region of interest (ROI), depicted as white square borders in Fig. 4 and the background. CNR can be defined as

$$CNR = \frac{contrast}{noise} = \frac{\Delta\mu}{noise} = \frac{\mu_{ROI} - \mu_{background}}{\sigma_{background}} \quad (27)$$

where μ_{ROI} is the mean value of the ROI; $\mu_{background}$ and $\sigma_{background}$ are the mean value and the standard deviation of the background area respectively.

We compute and compare the CNR for both proposed feature detector and the gradient-based edge detector at different contrast levels, shown in Fig. 5. It is obvious that the normalized Fisher-Tippett feature detector has higher CNR. It produces cleaner edge as it robustly identifies the important features without many false detections due to speckle.

Fig. 6 shows the registration error, both in translation and rotation. It is denoted as the squared error of the estimated parameter compared to the ground truth value. We can easily notice that the registration error of the gradient-based edge maps (solid blue curves) quickly increases as the contrast is diminished, while the registration error of the proposed method (dashed red curve) is significantly lower.

The only real parameter to the feature detector is the window size. Increasing the window size gives a better statistical modeling of the distribution's parameter in the window, and varies the scale of the feature detected. For example, in Fig. 7, we observe that the size of the features detected is proportional to the window size. Therefore, the window size affects the performance of registration, shown in Fig. 8.

Another example is shown in Fig. 10. The ground truth registration parameters are $(5,5)$ for the translation and 5° for the rotation. We use a feature detector of window size of 7×7 to compute the edge maps and compare the registration results to the gradient-based method. It is shown that the registration error of the proposed method is much lower, depicted in Fig. 9.

For the region image extracted from an abdominal part ultrasound image, we apply our method again to examine its effectiveness, using a feature detector of window size of 7×7, depicted in Fig. 11 and 12. Since there is no ground truth, we compute the sum of squared differences (SSD) between the original and registered images. The SSD decreased by 51.14% and 39.94% for the proposed method, while with the standard gradient scheme, the SSD decreased only by 12.73% and 0.35%.

5. CONCLUSION

In this article, we presented an ultrasound image registration scheme based on matching edge maps generated by a statistical feature detector based on theoretical distributions of fully formed speckle in an ultrasound image. Since the similarity metric is distribution to distribution comparison, rather than pixel-pixel intensity comparison, it is much more robust to uncorrelated speckle. Our experiments also demonstrate the ability of this method to accurately register ultrasound images, even for low contrast, speckled data, and showed how this method is more robust to noise than standard gradient-based methods.

The results presented in the paper indicate that the proposed method has much promise in robust registration of ultrasound data. Meanwhile, the proposed scheme is computationally efficient. Such kind of technique is a promising method to align speckled images for different applications in an ultrasound system. As future work, we are interested in the extended study to the cases where the speckle is not fully formed. Also, we will evaluate the proposed method for the next generation ultrasound machines.

REFERENCES

[1] B. Zitova and J. Flusser, "Image registration methods: A survey," *Image and Vision Computing*, vol. 21, no. 11, pp. 977-1000, 2003.

[2] J. B. Maintz and M. A. Viergever, "A Survey of Medical Image Registration," *Medical Image Analysis*, vol. 2, no. 1, pp. 1-36, 1998.

[3] Hajnal J., D. Hill, and D. Hawkes, *Medical Image Registration*, CRC Press, first edition, 2001.

[4] A. Goshtasby, *2-D and 3-D image registration for medical, remote sensing, and industrial applications*, J. Wiley and Sons, 2005.

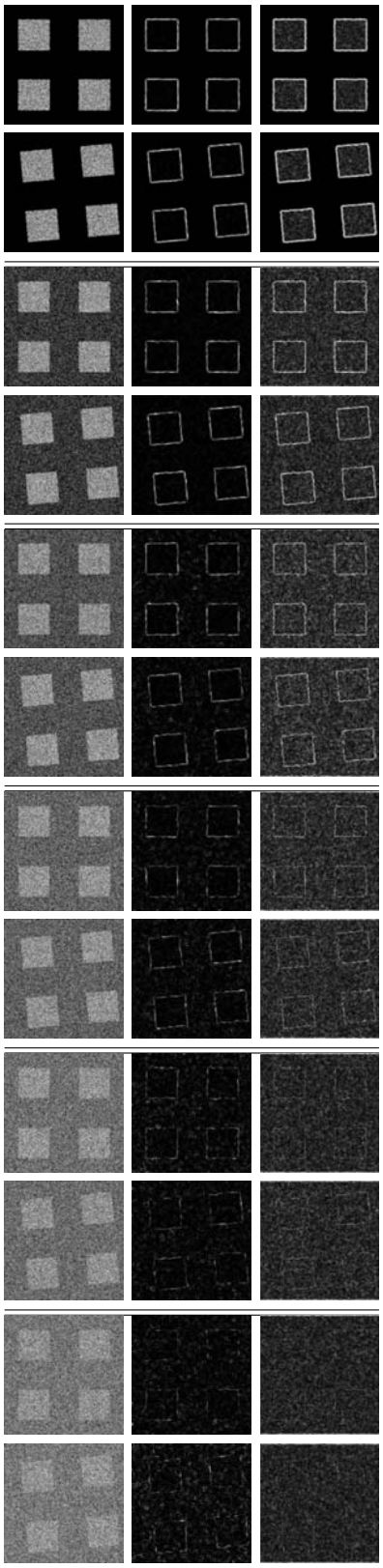

Fig. 3. Feature detection in synthetic ultrasound images. The leftmost column shows the original synthetic ultrasound images with diminishing contrast. The middle column shows the feature detection with information-theoretic method, while the rightmost column shows the feature detection with the difference of Gaussian filter.

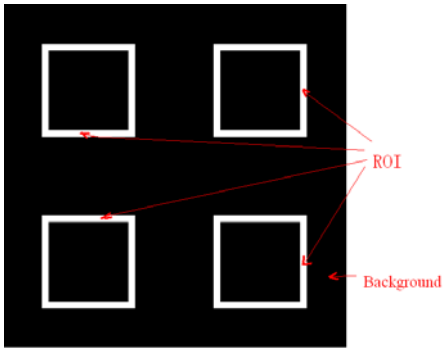

Fig. 4. Region of interest and the background

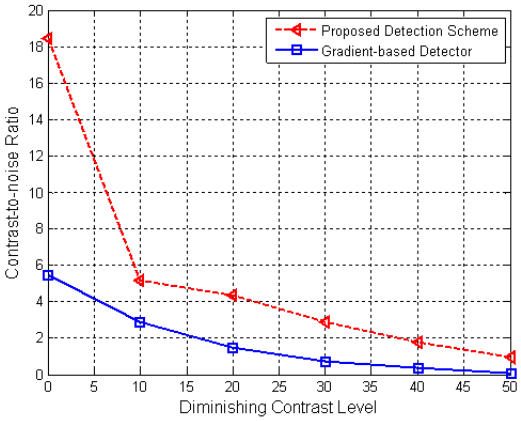

Fig. 5. CNR as a function of diminishing contrast.

[5] J. Modersitzki, *Numerical Methods for Image Registration*, Oxford Science Publications, Oxford, 2004.

[6] P. J. Besl and N. D. McKay, "A method for registration of 3D shapes," *IEEE Trans. Pattern Anal. Mach. Intell.*, vol. 14, no. 2, pp. 239-256, Feb. 1992.

[7] W. E. L. Grimson, D. P. Huttenlocher and T. D. Alter, "ecognizing 3D objects from 2D images: an error analysis," in *Proc. CVPR*, 1992, pp. 316-321.

[8] G. P. Penney, J. Weese, J. A. Little, P. Desmedt, D. L. G. Hill, and D. J. Hawkes, "A comparison of similarity measures for use in 2-D-3-D medical image registration," *IEEE Trans. Med. Imag.*, vol. 17, no. 4, pp. 586-595, Apr. 1998.

[9] G. Hermosillo, C. ChefdHotel, and O. Faugeras, "Variational Methods for Multimodal Image Matching," *International Journal of Computer Vision*, vol. 50, no. 3, pp. 329-343, 2002.

[10] E. DAgostino, F. Maes, D. Vandermeulen, and P. Suetens, "A viscous fluid model for multimodal nonrigid image registration using mutual information," in *Proc. Medical Image Computing and Computer-Assisted Intervention*, MICCAI 2002, pp.541-548, Tokyo, Japan, Sep. 2002.

[11] E. Haber and J. Modersitzki, "Intensity Gradient Based Registration and Fusion of Multi-modal Images," in *Proc. Medical Image Computing and Computer-Assisted Intervention*, MICCAI 2006, pp. 726-733, Copenhagen, Denmark, Oct. 2006.

[12] E. A. Gardner, T. S. Sumanaweera, M. N. Woelmer, R. W. Steins, E. Leen, "Removing local motion from ultrasonic images using nonaffine registration for contrast quantification," in *Proc. IEEE Ultrasonics Symposium*, vol. 3, pp. 1718-1721, Aug. 2004.

[13] V. Dutt and J. Greenleaf, "Statistics of the Log- Compressed Envelope," *Journal of the Acoustical Society of America*, vol. 99, no. 6, pp. 3817-3825, 1996.

[14] M. O'Donnell, A. R. Skovoroda, B. M. Shapo, and S. Y. Emelianov, "Internal Displacement and Strain Imaging Using Ultrasonic Speckle Tracking," *IEEE Trans. Ultrason., Ferroelect., Freq. Contr.*, vol. 41, no. 3, pp. 314-325, 1994.

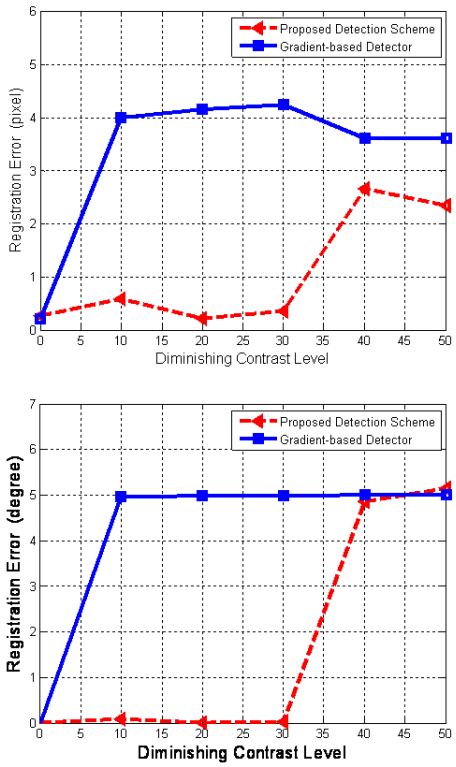

Fig. 6. Registration error as a function of diminishing contrast. The top figure shows the translational error while the bottom one shows rotational error.

[15] M. J. Ledesma-Carbayo, J. Kybic, M. Desco, A. Santos, M. Sühling, P. Hunziker, and M. Unser, "Spatio- Temporal Nonrigid Registration for Ultrasound Cardiac Motion Estimation," *IEEE Trans. Med. Imag.*, vol. 24, no. 9, pp. 1113-1126, 2005.

[16] B. Cohen and I. Dinstein, "New Maximum Likelihood Motion Estimation Schemes for Noisy Ultrasound Images," *Pattern Rec.*, vol. 35, no. 2, pp. 455-463, 2002.

[17] D. Boukerroui, J. A. Noble, and M. Brady, "Velocity Estimation in Ultrasound Images: a Block Matching Approach," in *Proc. Information Processing in Medical Imaging*, IPMI 2003, pp. 586-598, Ambleside, UK, Jul. 2003.

[18] Z. Wang, G. Slabaugh, G. Unal, M. Zhou and T. Fang, "An Information-Theoretic Detector Based Scheme for Registration of Speckled Medical Images," in *Proc. IEEE International Conference on Systems, Man, and Cybernetics*, SMC 2007, pp. 1026-1030, Montreal, Canada, Oct. 2007.

[19] G. Slabaugh, G. Unal and T. Chang, "Information-Theoretic Feature Detection in Ultrasound Images," in *Proc. IEEE International Conference of the Engineering in Medicine and Biology Society*, pp. 2638-2642, NYC, USA., Sep. 2006.

[20] M. Basu, "Gaussian-based edge-detection methods-a survey," in *IEEE Trans. Syst., Man, Cybern., Part C.*, vol. 32, no. 3, pp.252-260, Aug. 2002.

[21] J. Goodman, *Speckle Phenomena: Theory and Applications*, 1st ed. Work in Progress, 2005.

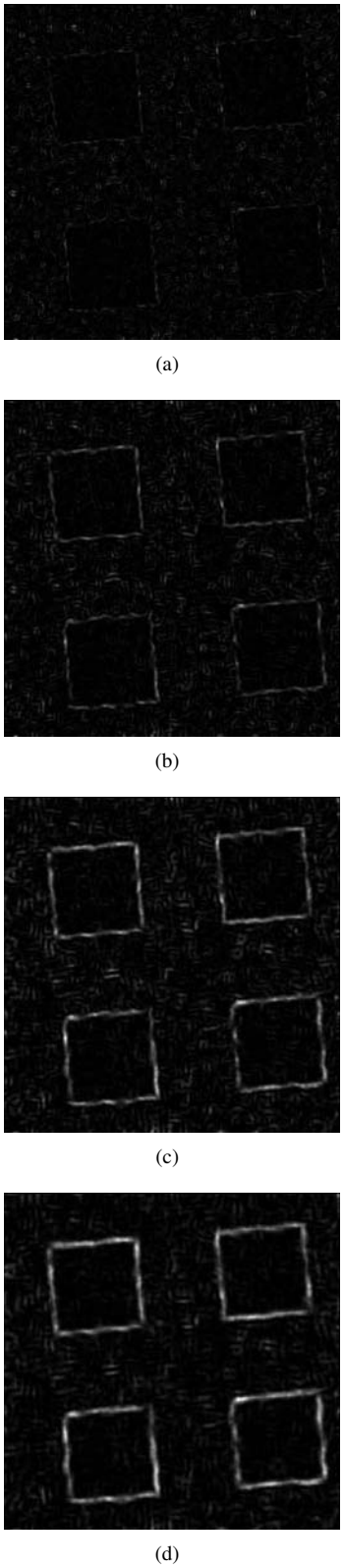

(a)

(b)

(c)

(d)

Fig. 7. Effect of window size to feature detection. From top to bottom : 3×3, 5×5, 7×7, 9×9.

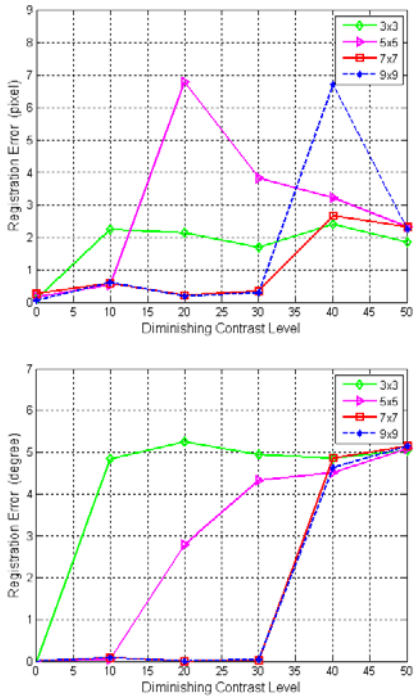

Fig. 8. Effect of window size to registration error as a function of diminishing contrast. The top figure shows the translational error while the bottom one shows rotational error.

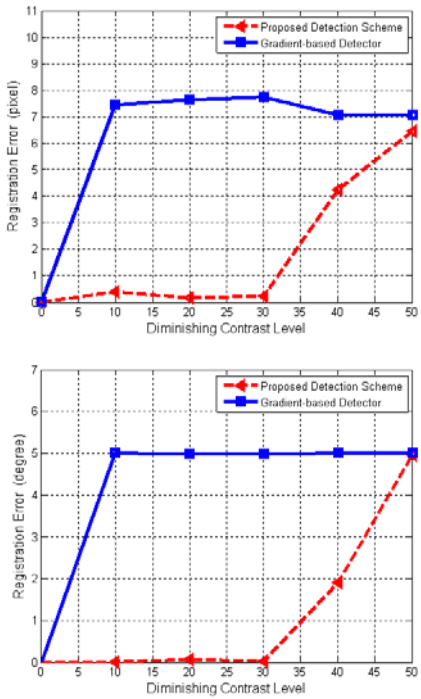

Fig. 9. Registration error as a function of diminishing contrast. The top figure shows the translational error while the bottom one shows rotational error.

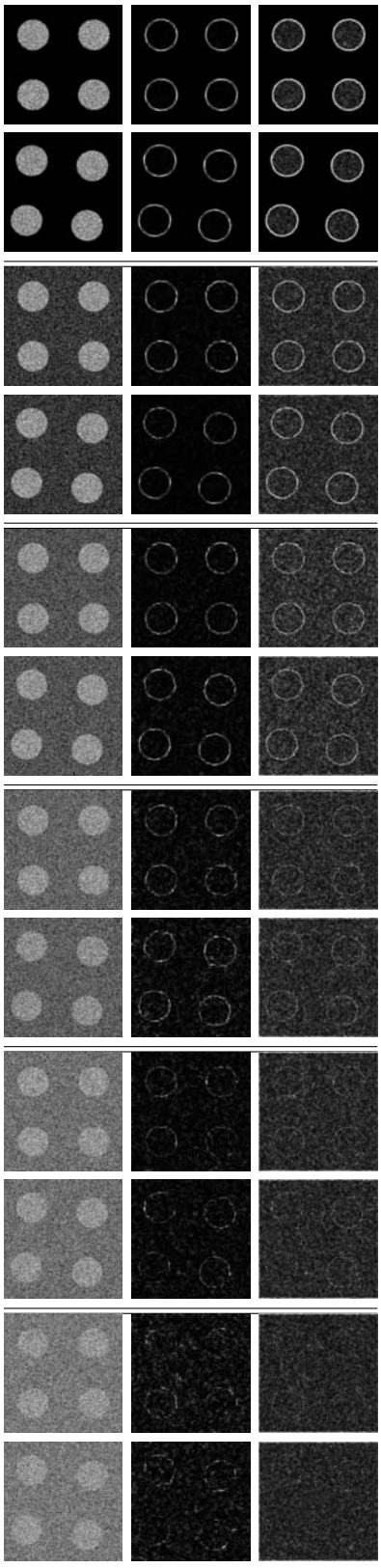

Fig. 10. Feature detection in synthetic ultrasound images. The leftmost column shows the original synthetic ultrasound images with diminishing contrast. The middle column shows the feature detection with information-theoretic method, while the rightmost column shows the feature detection with the difference of Gaussian filter.

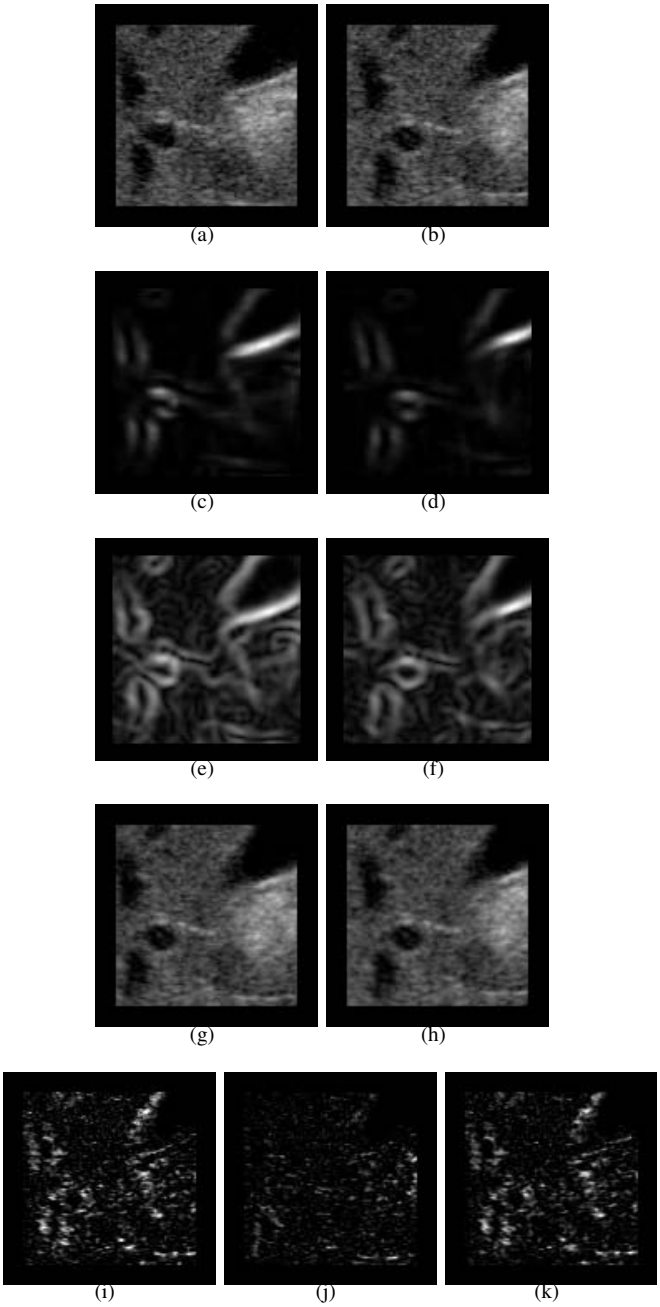

Fig. 11. Registration results of ultrasound images. Original (a)(b), feature detection with Fisher-Tippett (c)(d), gradient-based feature detection (e)(f), registered image with Fisher-Tippett and gradient detector (g)(h), original residue image (i), residue image with Fisher-Tippett detector (j), residue image with gradient detector (k).

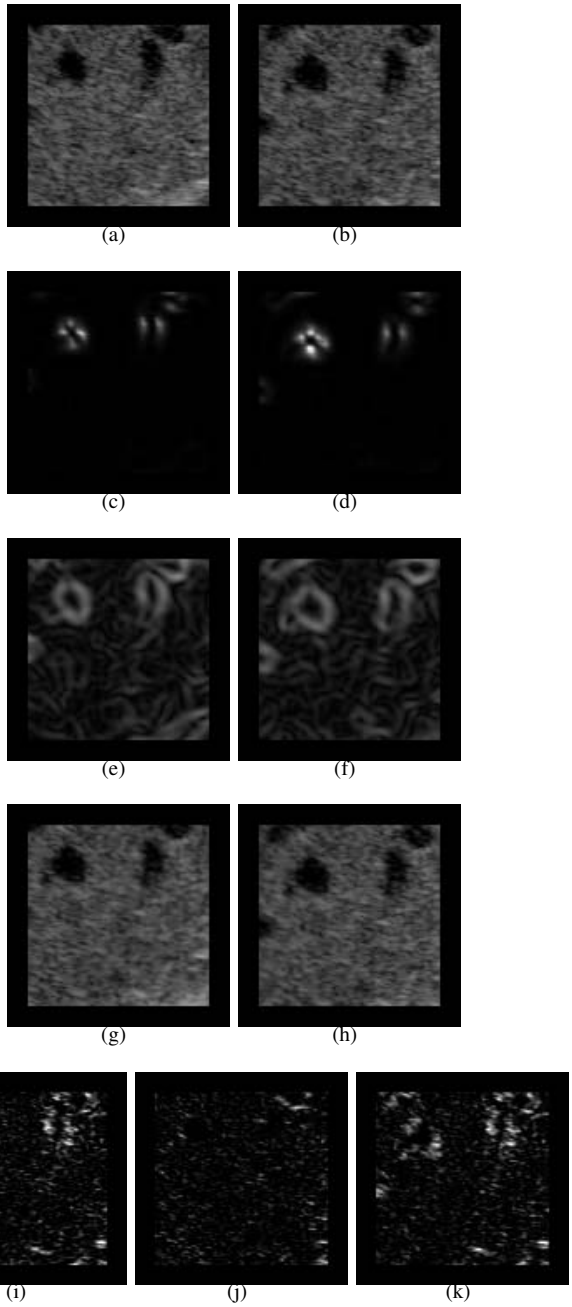

Fig. 12. Registration results of ultrasound images. Original (a)(b), feature detection with Fisher-Tippett (c)(d), gradient-based feature detection (e)(f), registered image with Fisher-Tippett and gradient detector (g)(h), original residue image (i), residue image with Fisher-Tippett detector (j), residue image with gradient detector (k).

Zhe Wendy Wang received the B.E. degree from Tsinghua University, China and M.E. degree from Chinese Academy of Science, both in electronics engineering. She is working towards her Ph.D. degree in the department of electrical and computer engineering, New Jersey Institute of Technology (NJIT), Newark. She has been working at Siemens Corporate Research, Princeton since July 2006. Her research interests include image segmentation, registration, filtering, object tracking and computer-aided diagnosis. Ms. Wang was the recipient of first place in the IEEE North Jersey Section Student Paper Presentation Contest(2008).

Gregory G. Slabaugh is the Head of Research and Development at Medicsight PLC, an industry leader in computer-aided detection software in medical imaging. Greg earned a PhD in Electrical Engineering from the Georgia Institute of Technology in Atlanta, GA, and also held positions at Hewlett-Packard Laboratories and Siemens Corporate Research. Greg is a Senior Member of IEEE and an Associate Editor of IEEE Signal Processing Magazine. He co-organized the International Workshop on Computer Vision for Intravascular and Intracardiac Imaging held in conjunction with MICCAI 2006, and served as a guest Associate Editor for a special issue of IEEE Transactions on Information Technology in Biomedicine on the same topic. Greg has over 40 publications and over 30 patents pending in the fields of computer vision and medical image processing; in particular, his research interests include computer-aided detection, image segmentation, registration, geometric modeling, multiview stereo, adaptive filtering, and partial differential equations.

Gozde Unal received the PhD degree in electrical engineering from North Carolina State University, Raleigh, in August 2002, She was as a postdoctoral fellow at the Georgia Institute of Technology in 2003 and visited HP Labs, Palo Alto, California, as a postdoctoral researcher during the summer of 2003. From Fall 2003 to 2007, she worked as a research scientist at Siemens Corporate Research, Princeton, New Jersey. She joined the faculty of Sabanci University, Istanbul, Turkey in Fall 2007, where she is currently an assistant professor. Her research interests include variational techniques with connection to information theory and probability theory, applications to various computer vision, and image processing problems such as stereoscopic camera calibration, 2D/3D image segmentation and registration, filtering and enhancement, and stochastic particle systems. Her current research is focused on medical image analysis, segmentation, registration, and shape analysis techniques with applications to clinically relevant problems in MR, CT, US, and intravascular images. She is a Senior Member of the IEEE, and Associate Editor for IEEE Transactions on Information Technology on Biomedicine.

Tong Fang received the Ph.D. degree in 2000 and the M.Sc degrees in electrical and computer engineering in 1999, industrial engineering in 1997 from Rutgers University, New Jersey. In 1992, he received the M.Sc degree in management science from University of Science and Technology, China. He is currently a research scientist and Manager of adaptive techniques R&D program at Siemens Corporate Research, Princeton, New Jersey. His current research interests include medical image processing, geometric modeling and visualization.